Penerbit Akademia Baru

Journal of Advanced Research in Experimental Fluid Mechanics and Heat Transfer

Journal homepage:
http://www.akademiabaru.com/submit/index.php/arefmht
ISSN: 2756-8202

AerospaAcer Valve-Holding Chamber Velocity Profile using Wind Tunnel Experiment

Riyadhthusollehan Khairulfuaad[1], Norzelawati Asmuin[1,*], Muhammad Kamal Arif Amir[1]

[1] Department of Aeronautic Engineering, Fakulti Kejuruteraan Mekanikal dan Pembuatan, Universiti Tun Hussein Onn Malaysia, 86400 Batu Pahat, Johor, Malaysia

ARTICLE INFO

Article history:
Received 20 April 2025
Received in revised form 10 May 2025
Accepted 15 June 2025
Available online 10 July 2025

Keywords:
Valve-holding chamber; pressurized meter-dose inhaler; aerodynamics internal flow behaviour

ABSTRACT

Millions of individuals worldwide suffer from asthma, a chronic inflammatory disease of the respiratory system. Although pressurized metered-dose inhalers (pMDIs) are widely used for asthma medication delivery, improper administration can lead to suboptimal drug delivery. To enhance medication deposition in the lungs, spacers, such as the AerospaAcer device, are employed to slow down aerosolized particles. This study investigates the aerodynamic performance of the AerospaAcer valve-holding chamber through wind tunnel experiments, focusing on various valve configurations, including the Duckbill and Cross-Slit valves. Wind tunnel testing was conducted at airflow rates of 30, 60, and 90 L/min, simulating typical inhalation conditions. Results revealed that the AerospaAcer with the Duckbill valve achieved the maximum pressure and velocity at the outlet, indicating optimal drug delivery potential. In contrast, the AerospaAcer without any valve configuration exhibited the highest pressure and velocity at the chamber's entrance. Drug particle retention rates were measured at 85.4%, demonstrating a 5% improvement over commercially available valve-holding chambers. Furthermore, the cylindrical design of the AerospaAcer combined with the Duckbill valve enhanced lower respiratory tract deposition by 3% compared to baseline VHC designs. These findings suggest that the AerospaAcer with a Duckbill valve can significantly improve drug delivery efficiency, reduce backflow, and enhance medication deposition in the lower respiratory tract. The data from this wind tunnel experiment provides valuable insights into the optimization of inhalation devices and their role in advancing respiratory drug delivery strategies.

1. Introduction

Asthma is a chronic respiratory disease that affects the airways in the lungs, causing them to become inflamed and narrowed. This condition could lead to a variety of symptoms, including wheezing, coughing, chest tightness, and difficulty breathing [1-5]. Asthma symptoms could range from mild to severe and may be triggered by various factors, such as allergens, respiratory infections, exercise, or exposure to irritants like smoke and pollutants [6,7]. Managing asthma typically involves

* *Corresponding author.*
E-mail address: norzela@uthm.edu.my

https://doi.org/10.37934/arefmht.21.1.182192

medications, lifestyle adjustments, and the use of devices like asthma inhalers and valve holding chambers to help individuals control their symptoms and maintain optimal lung function [6-10].

An asthma inhaler as shown in Figure 1, often referred to as a "puffer" or "rescue inhaler," is a medical device that delivers medication directly into the airways. Inhalers are commonly used by individuals with asthma to alleviate acute symptoms or to provide long-term control of asthma conditions [11-17]. These devices are portable, convenient, and deliver medication in aerosol form, allowing it to be inhaled into the lungs quickly, where it could provide rapid relief or reduce inflammation [18].

A valve holding chamber as shown in Figure 2, also known as a "spacer" or "aerosol spacer," is an accessory device used with inhalers to improve the delivery of medication, especially in individuals who may have difficulty coordinating their inhalation with the actuation of the inhaler. It is essentially a plastic or metal tube with one end attached to the inhaler and the other end having a mouthpiece or mask for the user to inhale from. The holding chamber helps ensure that the medication is properly dispersed and inhaled into the lungs, reducing the likelihood of medication being deposited in the mouth or throat [18,19].

Fig. 1. Inhaler devices [16]

Fig. 2. Inhaler attached to spacer device [4]

The inhalation control valve inside a valve holding chamber is a critical component designed to optimize the delivery of medication from the inhaler to the user's lungs. This valve typically opens when the individual inhales through the mouthpiece or mask, allowing the medication to be released from the chamber and into the airway. When the user exhales, the valve closes, preventing medication from escaping and ensuring that it remains available for inhalation during the next breath. This valve improves the coordination between inhaler activation and inhalation, making it easier for individuals, especially children and those with compromised lung function, to receive the full benefit of their asthma medication.

In summary, asthma is a chronic respiratory disease characterized by airway inflammation and constriction, and its management often involves the use of asthma inhalers and valve holding chambers. These devices help individuals with asthma effectively administer their medication and achieve better control of their symptoms. The inclusion of an inhalation control valve within the valve holding chamber enhances the delivery of medication, making it more accessible and efficient for users.

Conducting wind tunnel experiments on the internal aerodynamic flow inside an asthma valve holding chamber using a Pitot tube and an anemometer device could provide valuable insights into how airflow behaves within the chamber. This approach allows for precise measurements of airflow velocity and pressure, aiding in the optimization of the chamber's design for effective medication delivery. The primary objective of wind tunnel experiments with a Pitot tube and anemometer in the

context of an asthma valve holding chamber is to study the airflow patterns, velocity, and pressure distribution within the chamber. These experiments aim to assess the chamber's performance and provide data for improving its design [20].

2. Methodology

The present study is divided into two (2) parts, model fabrication process and experimental process. In the fabrication process, all parts of AerospaAcer were fabricated with 3D print technology. The only parts that are not fabricated are the chamber as a cylindrical plexiglass was used according to Abd Rahman *et al.,* [4]. In an experimental process, an AerospaAcer's stand used to secure AerospaAcer inside wind tunnel was fabricated using steel with various shapes and dimensions. By using welding processes, the steel material is assembled as needed.

2.1 Fabrication Process

2.1.1 AerospaAcer prototype

There were five (5) parts in the fully assembled AerospaAcer prototype. These consist of feeder cap, chamber, mouth cap, control valve, and valve casing. The feeder cap, mouth cap, control valve and valve casing were fabricated using 3D print technology while the chamber was using existing cylindrical plexiglass. All printed parts as shown in Figure 3 and Figure 4 were drawn using computer aided design software known as Solidworks version 2022 before transferred to slicer software known as Flashprint version 5. The slicer software was used specifically to create a. gcode file format for Flash Forge Creator Pro 3D printer machine.

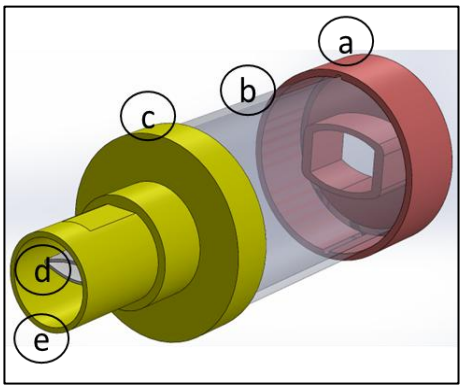

Fig. 3. AerospaAcer parts (a) Feeder cap (b) Chamber (c) Mouthpiece (d) Control valve (e) Valve casing

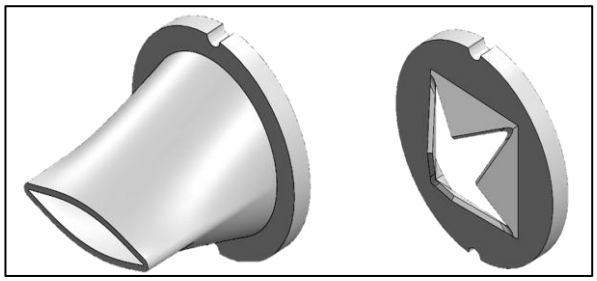

(a) (b)

Fig. 4. Control valves use for two (2) from three (3) AerospaAcer models (a) Duckbill valve (b) Cross-slit valve

Each part of AerospaAcer was printed with different material as shown in Figure 5. To provide a rigid structure while having a firm grip on asthma inhaler, feeder cap is 3D printed using thermoplastic polyurethane, TPU filament materials. Mouth cap and valve casing which needed to be strong enough to hold onto the chamber and protect valve from damage, hence it was printed using polylactic acid, PLA 3D printer filament. The soft and elastic properties of thermoplastic elastomer, TPE 3D printer filament material was used to print the control valve.

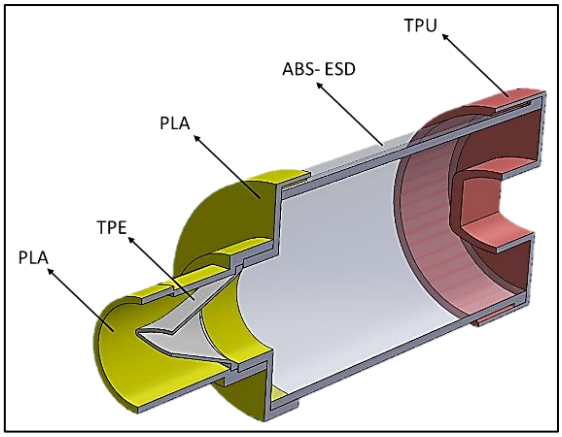

Fig. 5. Cross sectional of AerospaAcer

2.1.2 AerospaAcer stand for wind tunnel

Securing AerospaAcer firmly inside the wind tunnel is crucial. Hence, an AerospaAcer Stand was fabricated to hold the prototype model inside the wind tunnel as shown in Figure 6. The AerospaAcer Stand was fabricated using 304.8 mm x 304.8 mm of 3 mm thick steel plate as base and a 60 mm x 1.6 mm cylindrical bar to hold AerospaAcer in place. The AerospaAcer is raised from the stand base at 197 mm to position it at the middle of wind tunnel using 12.7 mm x 12.7 mm with 1 mm thickness hollow steel bar as pillars for AerospaAcer prototype model. The same dimension of steel bar is also used for pitot tube hold it in middle of AerospaAcer. All materials were welded together according to desired positions. The AerospaAcer stand is also built with a set of nuts and bolt at the bottom of its base steel plate. These nuts and bolts were meant to secure the stand inside wind tunnel so it would not vibrate and misplaced by itself during experimental procedure is started.

Fig. 6. AerospaAcer stand used to hold AerospaAcer inside wind tunnel

2.2 Experimental Process

The experiment was conducted using a wind tunnel instrument with 6.1 m long and 2 m height as shown in Figure 7. This wind tunnel includes a test section, a diffuser, a blower, a contraction cone,

and three (3) screens arranged in a settling chamber. The test section has a cross-section of 400 mm x 400 mm and length of 1250 mm. To provide a smooth transition of air from low to atmospheric pressure via volume expansion, the diffuser is positioned at the conclusion of the test segment. Prior to the airflow leaving the diffuser, it helps to reduce wind speed. The fan is housed in the driver area, which is situated at the diffuser outlet. The fan has a maximum power of 10 HP and a total of 14 pieces of blades with freestream velocities of less than 40 m/s.

Fig. 7. Wind tunnel instrument

In order to determine the velocity pressure, which is subsequently used to determine air velocity, a Pitot tube in Figure 8(a) is utilized to detect both the static and total pressures. After being introduced into the duct, the Pitot tube's tip is placed such that it faces the direction of the airflow. It was then attached to the rubber tube connected to the anemometer as shown in Figure 8(b). This was set up intentionally to measure air velocity and pressure inside the AerospaAcer secured inside wind tunnel earlier as shown in Figure 8(c). A calibration of pitot tube and anemometer was done based on data specification provided with the wind tunnel instrument.

The experiment was started by slowly increasing the speed knob on the wind tunnel inverter speed controller. The inverter is set to produce 10 Hz for the first reading of measurement. As the wind tunnel rotor had achieved its stable rotation, air flow velocity and pressure at AerospaAcer inlet was recorded according to anemometer reading. This procedure was repeated for all AerospaAcer model i.e., no valve, duckbill, and cross slit model until the frequency is set on inverter is 30 Hz with 5 Hz increment.

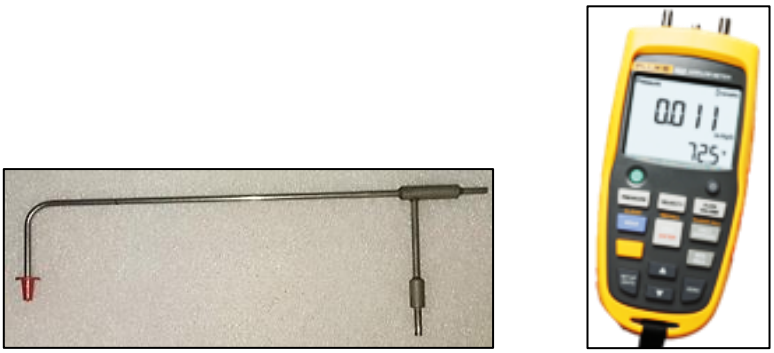

(a) (b)

Fig. 8. Wind tunnel experiment (a) Pitot tube (b) Anemometer

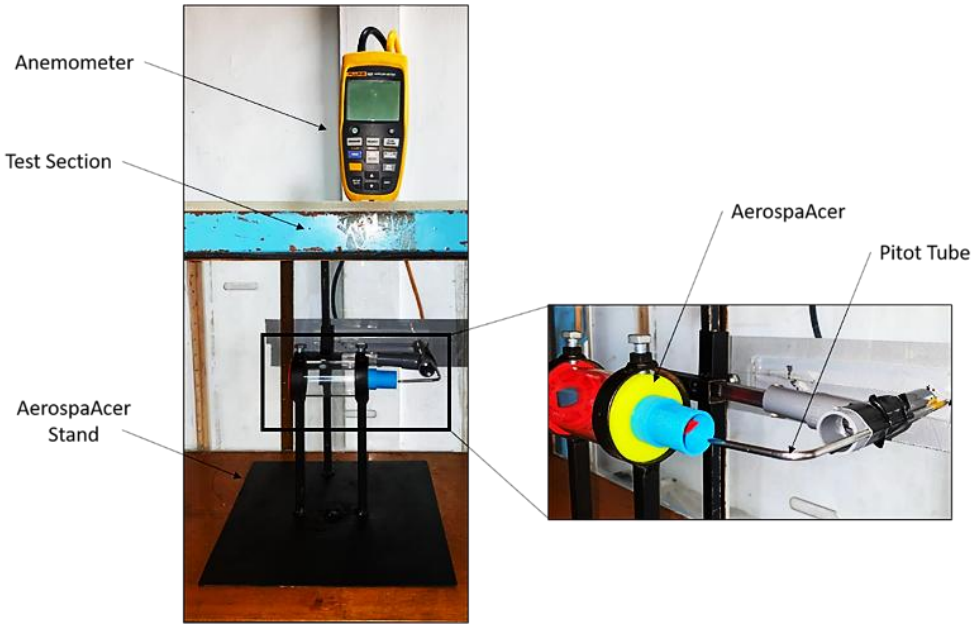

(c)

Fig. 8. Wind tunnel experiment (c) Equipment and instrumental setup

3. Results

3.1 Velocity and Pressure

3.1.1 Inlet

Figure 9 shows the velocity level at inlet of AerospaAcer at fives (5) different level of revolution per minutes set on wind tunnel inverter. The velocity for all three (3) AerospaAcer' model configurations, according to the general trend presented in Figure 9 demonstrates a positive association with revolutions per minute, with a linear increase observed. This suggests that as the revolution per minute of wind tunnel rotor rises, so will the fluid flow rate through the model. The initial velocity at inlet of AerospaAcer for duckbill and cross-slit having slightly different where duckbill produced lower inlet velocity than cross-slit with 1.869 m/s and 2.489 m/s respectively. No-valve, however, produced higher inlet velocity at 10 Hz recorded at 5.839 m/s. The maximum inlet velocity-revolution per minute relation occurred on duckbill model is recorded as lowest with all velocity ranging below 4.607 m/s for all revolution per minute increment.

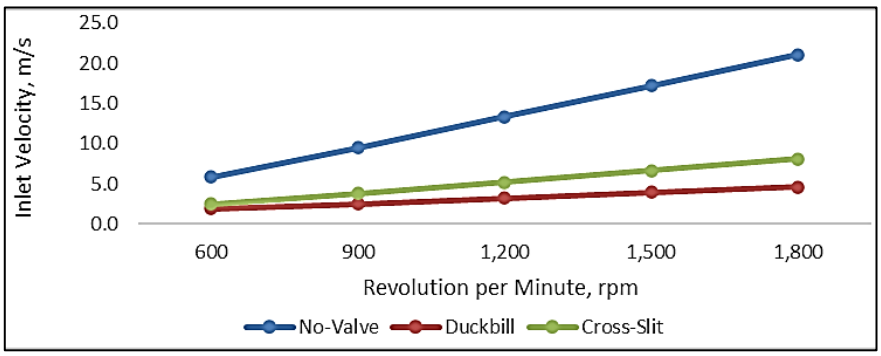

Fig. 9. Graph of inlet velocity, m/s against revolution per minute, rpm

Furthermore, maximum velocity- revolution per minute relation for cross-slit model formed second highest as it tops at 8.122 m/s. Hence, this model creates intermediate increment of velocity throughout the constant increasing of revolution per minute created by win tunnel's inverter. No-

valve model produced the highest maximum velocity- revolution per minute relationship peaked at 21.066 m/s. These show that duckbill configuration as a control valve could slow down the high velocity of air flows inside an AerospaAcer. Cross-slit becomes the second best to decrease the fast inlet velocity of air flows while no-valve model falls as third. In Figure 10, there was a big difference of pressure values between the rising inlet air pressure of no-valve model and low pressure of the valved models. No-valve model produced bigger pressure different as the revolution per minute of wind tunnel rotor gets higher. Both duckbill and cross-slit model, however, create low pressure even though the revolution per minute was set to highest level during experiment.

A slight curve of pressure reading happens between 600 rpm and 1,200 rpm for no-valve models before it went linearly increase as high as 256.6 Pa at 1,800 rpm. Initially, duckbill was recorded to produced inlet pressure of 2 Pa lower than cross-slit which produced 4 Pa. The same scenario happens at 900rpm where only a small difference of 5 Pa in which duckbill still produced lower inlet pressure than cross-slit. As the rpm was set to increase, the inlet pressure for cross-slit gradually increased where 39.4 Pa as it peaks. The inlet pressure produced by duckbill only gets higher than 10Pa when the revolution per minutes had reach 1,800 rpm. However, it is still considered as the lowest pressure among all three (3) models with only 12.6 Pa at this point.

According to these findings, it was clear that duckbill model creates lowest inlet pressure among all three (3) models experimented. This was followed by cross-slit with maximum inlet pressure recorded below 40 Pa. The high inlet pressure created by the no-valve model shows that a control valve inside AerospaAcer is needed to produce low pressure.

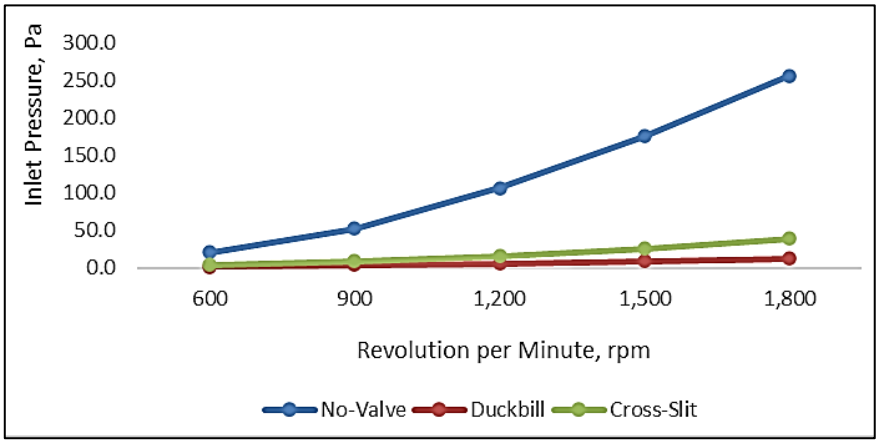

Fig. 10. Graph of inlet pressure, Pa against revolution per minute, rpm

3.1.2 Outlet

In general, it is clear from analyzing the graph of velocity against revolution per minute in Figure 11 that the duckbill and cross-slit valves show similar patterns in terms of velocity variations with revolution per minute. As the frequency rises, the velocity is linearly increased for both valve configurations. This implies that both valves efficiently enable fluid flow and sustain a constant velocity across a broad frequency range. The no-valve model, however, exhibits a different behavior. Initially, the velocity also rises linearly with revolution per minute between 600 rpm and 900 rpm slightly higher than Cross-Slit model. However, it starts to fall below Cross-Slit for 1,200 rpm until 1,800 rpm. Through these outcomes, it suggests that the flow in the absence of a valve is subject to free outflows that result in a drop in velocity at higher RPM.

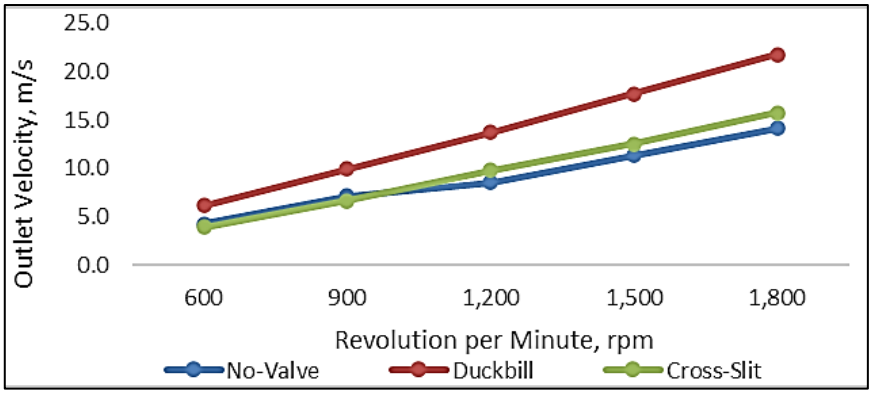

Fig. 11. Graph of outlet velocity, m/s against revolution per minute, rpm

In Figure 12, graph of outlet pressure, Pa against revolution per minute, rpm is shown. According to the recorded data, duckbill model shown the highest outlet pressure for all five (5) RPM. The high outlet pressure produced by duckbill model spans from minimum of 22.6 Pa to the maximum at 283.0Pa. No-valve model produced an intermediate outlet pressure during 600rpm and 900 rpm at 10.6 Pa and 30.6 Pa respectively. This trend changed as the RPM hit 1,200 rpm where the no-valve model produced lower outlet pressure than cross-slit which makes it the lowest among the three. It continues to be the lowest until RPM reaches 1,800rpm with its maximum value tops at 117.2 Pa only.

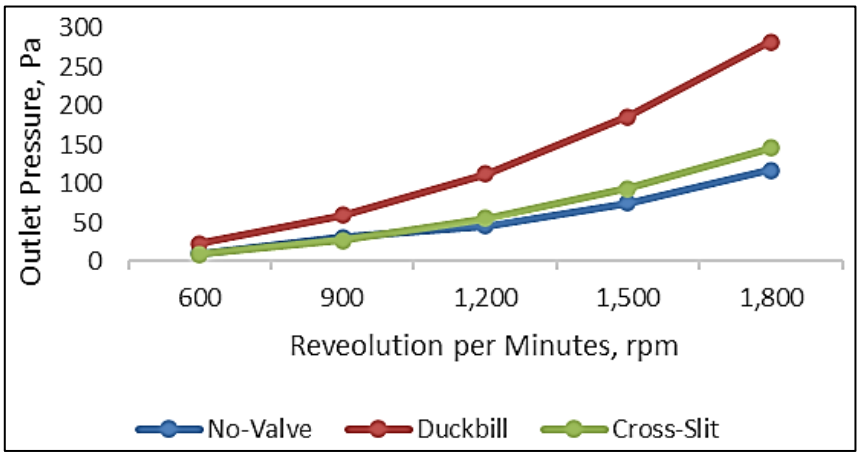

Fig. 12. Graph of outlet pressure, Pa against revolution per minute, rpm

3.2 Reynold Number

Overall, based on Figure 13 there was no laminar flow recorded among all three inlets of AerospaAcer models. All Reynolds numbers were either transitional flows or turbulence flow in which it increases as the revolution of rotor is gradually increased. No-valve models produced the highest Reynolds number with turbulence flow for all RPM levels. This is followed by the cross-slit model while Duckbill produced the least Reynolds number. A high *Re*-created by No-Valve model recorded at 6,999.41 initially is progressively gets bigger with higher revolution per minutes. The maximum measured *Re* peaks at 25,252.55 as the RPM reaches 1,800 rpm. Duckbill models produced the smallest range of inlet Reynolds numbers at transitional flows for 600 rpm, 900 rpm, and 1,200 rpm with 2,240.44, 2,954.88, and 3,828.76, respectively. It was not until the revolution per minutes reached 1,500 rpm, Duckbill models start to give a turbulence flows with 4,736.20 while 1,800 rpm give 5,522.57 Reynolds numbers.

An intermediate series of data was documented by cross-slit model at all levels of RPM. Cross-slit starts with a transitional flow of 2,983.65 at 600 rpm. It was then changed to turbulence flow for 900 rpm until 1,800 rpm with its highest *Re* at 9,736.12. Generally, Duckbill model produced biggest differences between inlet and outlet Reynolds number followed by cross-slit model and no-valve model. According to the same Figure 14, each valved model creates a higher outlet Reynolds number than inlet. The non-valved model, however, creates contradictory data from the valved models with outlet Reynolds number is smaller than its inlet.

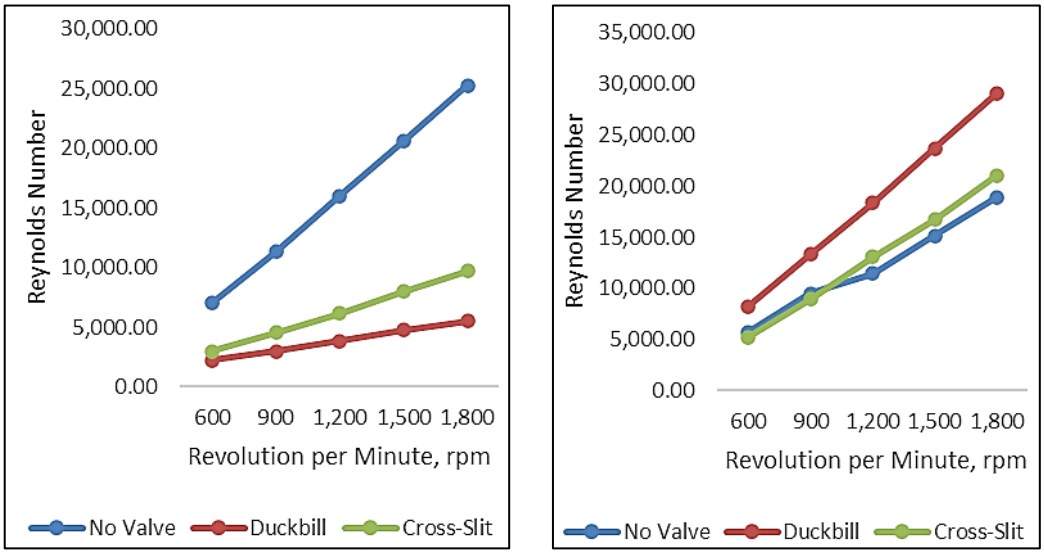

(a) (b)

Fig. 13. Graph against revolution per minute, rpm (a) Inlet Reynolds number (b) Outlet Reynolds number

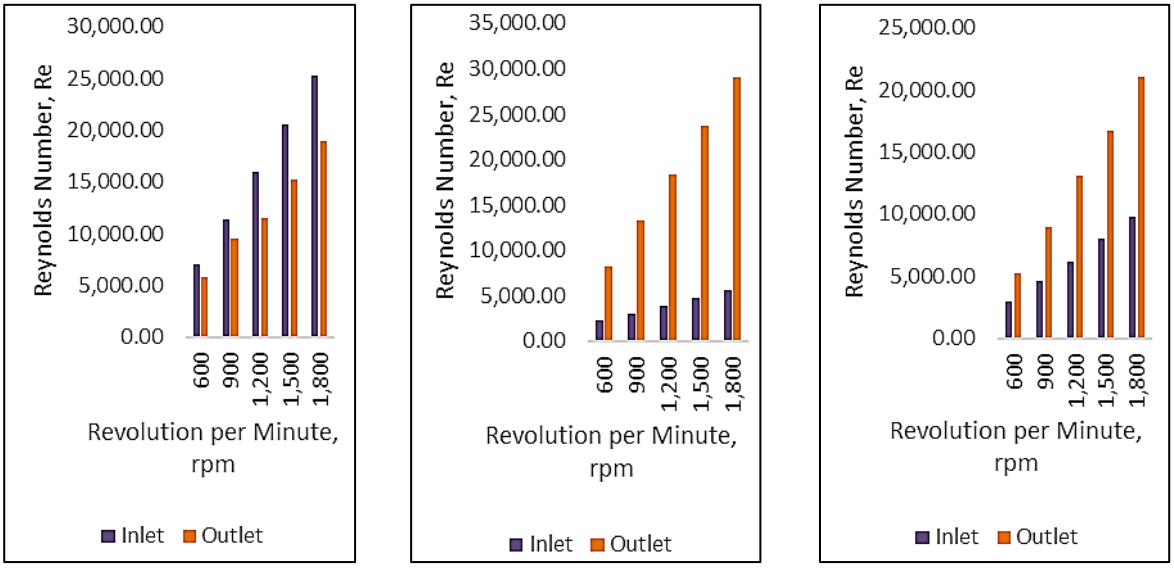

(a) (b) (c)

Fig. 14 Graph of comparison between inlet and outlet of Reynolds number against revolution per minute, rpm (a) No-valve (b) Duckbill (c) Cross-slit model

3.3 Pressure Drop

In Figure 15, the graph shows the pressure drop of all three (3) models produced during the experiment. As shown in the figure, Duckbill model creates the highest pressure drop for each revolution set. This was followed by the No-valve model as the second highest and cross-slit model creates the lowest pressure drop among all models experimented. A slight difference of pressure drop occurred between no-valve and cross-slit model at 600 rpm and 900 rpm with only 4.6 rpm of a difference for both revolutions.

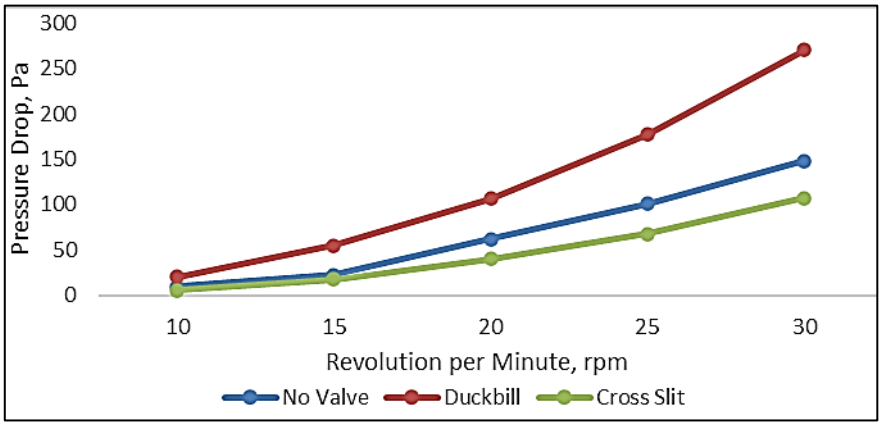

Fig. 15. Graph of pressure drop, Pa against revolution per minute, rpm

4. Conclusions

In conclusion, the No-valve model creates the highest flow rate followed by cross-slit and Duckbill model. Due to its design, which increases resistance to fluid flow, the Duckbill model demonstrated the slowest internal flow among all three (3) models studied. The cross-slit model had roughly balanced inlet and exit velocities, resulting in faster flow compared to the Duckbill model. The no-valve arrangement had the highest inlet velocity and the fastest fluid flow. These results underline how crucial it is to consider fluid dynamics and control valve design when choosing spacer devices for respiratory treatment. The duckbill valve displayed the slowest fluid flow among the three valve types. This is a result of the duckbill valve's flexible slit's design, which opens when pressure is applied and closes when pressure is withdrawn. In comparison to the other arrangements, this design causes fluid flow to encounter resistance, lengthening the transit time which is beneficial for tidal respiratory problems such as asthma.

Acknowledgement

Communication of this research is made possible through monetary assistance by Universiti Tun Hussein Onn Malaysia and the UTHM Publisher's Office via Publication Fund E15216. This research also under internal grant of Research Enhancement-Graduate Grant (REGG Q047).

References

[1] Amini, Shahideh, Arezou Ghasemi, Mohammad Solduzian, Besharat Rahimi, Kazem Heidari, Molouk Hadjibabaie, and Mona Kargar. "Is inhaler technique associated with quality of life in patients with chronic obstructive pulmonary disease?." *Current Therapeutic Research* 93 (2020): 100608. https://doi.org/10.1016/j.curtheres.2020.100608

[2] Higenbottam, Tim, Tom Siddons, and Eric Demoncheaux. "The direct and indirect action of inhaled agents on the lung and its circulation: lessons for clinical science." *Environmental Health Perspectives* 109, no. suppl 4 (2001): 559-562. https://doi.org/10.1289/ehp.01109s4559

[3] Jeswani, Harish Kumar, and Adisa Azapagic. "Life cycle environmental impacts of inhalers." *Journal of Cleaner Production* 237 (2019): 117733. https://doi.org/10.1016/j.jclepro.2019.117733

[4] Abd Rahman, Muhammad Faqhrurrazi, Nor Zelawati Asmuin, Ishkrizat Taib, Mohamad Nur Hidayat Mat, and Riyadhthusollehan Khairulfuaad. "Influence of actuator nozzle angle on the flow characteristics in pressurized-metered dose inhaler using CFD." *CFD Letters* 12, no. 6 (2020): 67-79. https://doi.org/10.37934/cfdl.12.6.6779

[5] Abd Rahman, Muhammad Faqhrurrazi, Suzairin MD Seri, Nor Zelawati Asmuin, Ishkrizat Taib, and Nur Syakirah Rabiha Rosman. "Response surface methodology (RSM) approach for optimizing the actuator nozzle design of pressurized metered-dose inhaler (pMDI)." *CFD Letters* 13, no. 7 (2021): 27-44. https://doi.org/10.37934/cfdl.13.7.2744

[6] Bateman, Eric D., Suzanne S. Hurd, Peter J. Barnes, Jean Bousquet, Jeffrey M. Drazen, Mark FitzGerald, Peter Gibson, K. Ohta, P. O'Byrne, S.E. Pedersen, E. Pizzichini, S.D. Sullivanee, S.E. Wenzel, and H.J. Zar. "Global strategy for asthma management and prevention: GINA executive summary." *European Respiratory Journal* 31, no. 1 (2007): 143-178. https://doi.org/10.1183/09031936.00138707

[7] Pope III, C. Arden, Joseph B. Muhlestein, Heidi T. May, Dale G. Renlund, Jeffrey L. Anderson, and Benjamin D. Horne. "Ischemic heart disease events triggered by short-term exposure to fine particulate air pollution." *Circulation* 114, no. 23 (2006): 2443-2448. https://doi.org/10.1161/CIRCULATIONAHA.106.636977

[8] Anderson, Gregor, Neil Johnson, Aruni Mulgirigama, and Bhumika Aggarwal. "Use of spacers for patients treated with pressurized metered dose inhalers: focus on the VENTOLIN™ Mini Spacer." *Expert Opinion on Drug Delivery* 15, no. 4 (2018): 419-430. https://doi.org/10.1080/17425247.2018.1437414

[9] Ramesh, Navitha, Fernando Holguin, and Sandhya Khurana. "High-Risk Asthma Clinic: Putting It All Together." *Difficult to Treat Asthma: Clinical Essentials* (2020): 297-311. https://doi.org/10.1007/978-3-030-20812-7

[10] Sukri, Nursyuhada, Siti Nurkamilla Ramdzan, Su May Liew, Hani Salim, and Ee Ming Khoo. "Perceptions of childhood asthma and its control among Malays in Malaysia: a qualitative study." *NPJ Primary Care Respiratory Medicine* 30, no. 1 (2020): 26. https://doi.org/10.1038/s41533-020-0185-z

[11] Ammari, Wesam G., Ghaleb A. Oriquat, and Mark Sanders. "Comparative pharmacokinetics of salbutamol inhaled from a pressurized metered dose inhaler either alone or connected to a newly enhanced spacer design." *European Journal of Pharmaceutical Sciences* 147 (2020): 105304. https://doi.org/10.1016/j.ejps.2020.105304

[12] Burudpakdee, Chakkarin, Vladimir Kushnarev, Dominic Coppolo, and Jason A. Suggett. "A retrospective study of the effectiveness of the AeroChamber Plus® Flow-Vu® Antistatic Valved Holding Chamber for asthma control." *Pulmonary Therapy* 3 (2017): 283-296. https://doi.org/10.1007/s41030-017-0047-1

[13] Kerwin, Edward M., Andrew Preece, Dimitra Brintziki, Kathryn A. Collison, and Raj Sharma. "ELLIPTA dry powder versus metered-dose inhalers in an optimized clinical trial setting." *The Journal of Allergy and Clinical Immunology: In Practice* 7, no. 6 (2019): 1843-1849. https://doi.org/10.1016/j.jaip.2019.02.023

[14] McIvor, R. Andrew, Hollie M. Devlin, and Alan Kaplan. "Optimizing the delivery of inhaled medication for respiratory patients: the role of valved holding chambers." *Canadian Respiratory Journal* 2018, no. 1 (2018): 5076259. https://doi.org/10.1155/2018/5076259

[15] Nicola, Mina, Youssef MA Soliman, Raghda Hussein, Haitham Saeed, and Mohamed Abdelrahim. "Comparison between traditional and nontraditional add-on devices used with pressurised metered-dose inhalers." *ERJ Open Research* 6, no. 4 (2020). https://doi.org/10.1183/23120541.00073-2020

[16] Schreiber, Jens, Tina Sonnenburg, and Eva Luecke. "Inhaler devices in asthma and COPD patients–a prospective cross-sectional study on inhaler preferences and error rates." *BMC Pulmonary Medicine* 20 (2020): 1-12. https://doi.org/10.1186/s12890-020-01246-z

[17] Tarlo, Susan M, Olivier Vandenplas, David I Bernstein, and Jean-Luc Malo. *Asthma in the workplace: Fifth edition*. Taylor & Francis Group, 2021. https://doi.org/10.1201/9781003000624

[18] Vincken, Walter, Mark L. Levy, Jane Scullion, Omar S. Usmani, PN Richard Dekhuijzen, and Chris J. Corrigan. "Spacer devices for inhaled therapy: why use them, and how?." *ERJ Open Research* 4, no. 2 (2018). https://doi.org/10.1183/23120541.00065-2018

[19] Lavorini, Federico, Celeste Barreto, Job FM van Boven, Will Carroll, Joy Conway, Richard W. Costello, Birthe Hellqvist Dahl, Richard P.N. Dekhuijzen, Stephen Holmes, Mark Levy, Mathieu Molimard, Nicholas Roche Miguel Román-Rodriguez, Nicola Scichilone, Jane Scullion, and Omar S. Usmani. "Spacers and valved holding chambers—the risk of switching to different chambers." *The Journal of Allergy and Clinical Immunology: In Practice* 8, no. 5 (2020): 1569-1573. https://doi.org/10.1016/j.jaip.2019.12.035

[20] Herrera, Ivan A. *The design, construction, and analysis of an open-circuit wind tunnel*. Honors Program diss., California State University, 2021.